

Numerical simulation of the evolution of glacial valley cross sections

HAKIME SEDDIK*

RALF GREVE

SHIN SUGIYAMA

Institute of Low Temperature Science, Hokkaido University,
Kita-19, Nishi-8, Kita-ku, Sapporo 060-0819, Japan

RENJI NARUSE

Glacier and Cryospheric Environment Research Laboratory,
Higashi-machi 2-339, Tottori 680-0011, Japan

Abstract

A numerical model was developed for simulating the formation of U-shaped glacial valleys by coupling a two-dimensional ice flow model with an erosion model for a transverse cross section. The erosion model assumes that the erosion rate varies quadratically with sliding speed. We compare the two-dimensional model with a simple shallow-ice approximation model and show the differences in the evolution of a pre-glacial V-shaped valley profile using the two models. We determine the specific role of the lateral shear stresses acting on the glacier side walls in the formation of glacial valleys. By comparing the model results with field data, we find that U-shaped valleys can be formed within 50 ka. A shortcoming of the model is that it primarily simulates the formation of glacial valleys by deepening, whereas observed valleys apparently have formed mainly by widening.

1 Introduction

Despite the fact that U-shaped valleys are characteristic products of alpine glaciation, the interaction of ice flow and glacial erosion which creates such well-known glacial forms has not been widely studied. Empirical studies have established the general concept that many glaciated valleys have approximately parabolic (U-shaped) cross sections (Graf, 1970; Doornkamp and King, 1971; Girard, 1976; Aniya and Welch, 1981). Both the development of numerical ice-flow models (Reynaud, 1973; Budd and Jensen, 1975; Mahaffy, 1976; Hook and others, 1979; Iken, 1981; Bindschadler 1982; Oerlemans, 1984) and the theoretical and empirical work in geomorphology (Hallet, 1979, 1981; Shoemaker, 1988; Iverson, 1990,

*E-mail: hakime@lowtem.hokudai.ac.jp

1991) have improved the capability to simulate the characteristics of glacier motion and the understanding of glacial erosion processes at small scales.

While previous valley evolution studies from Harbor (1990, 1992, 1995) and MacGregor and others (2000) have provided a better geomorphological understanding of glacial valley formation, little has been done to investigate the glaciological processes involved in their formation. The glacial cross section evolution model used by Harbor (1990, 1992) successfully simulated a proper erosion pattern (central minimum in the basal sliding velocity) for the U-shaped channel development by assuming a quadratic function of the sliding velocity for the erosion law, and it has identified the drag process associated with it. However, Harbor (1990, 1992) provided little information on the computation of the basal shear stress, which is required for successful erosion modeling. In particular, the detailed stress conditions required for the development of a U-shaped valley have not been described. Our work is complementary to the Harbor study and describes how the lateral shear stress affects the development of glacial valleys.

In this paper, we present the details of the two-dimensional flow pattern computation and its coupling with the subglacial erosion model. The study focuses in particular on the investigation of the influence of the lateral shear stress component on the formation of a U-shaped valley. For this purpose, the two-dimensional model is compared with a simple shallow-ice model in order to highlight the glacier stress conditions favorable to the formation of U-shaped valleys. Moreover, an attempt is made to constrain the basal sliding parameter by comparing the model results with glacial valley field data.

2 Methods

We developed a two-dimensional ice flow model in a transverse section and coupled it to an erosion model. The flow model solves the velocity field in a transverse cross section of a glacier assuming a uniform geometry along the glacier. We used a Cartesian coordinate with the x -axis along the glacier, y across the glacier, and z perpendicular to the x - y plane pointing upward (Fig. 1a). The stress components are τ_{xx} , τ_{yy} , τ_{zz} , τ_{xy} , τ_{xz} , τ_{yz} . All elements move along lines parallel to the x -axis, so that the only velocity component is u . We are interested in how u varies with y and z and so assume that it does not depend on x . These assumptions imply that the strain rates $\dot{\epsilon}_x$, $\dot{\epsilon}_y$, $\dot{\epsilon}_z$, $\dot{\epsilon}_{yz}$ are all zero. It follows that the stress-deviator components τ_{xx}^D , τ_{yy}^D , τ_{zz}^D , τ_{yz}^D are all zero, and the equilibrium equation for the momentum balance of the ice in the x direction is (Nye, 1965)

$$\frac{\partial \tau_{xy}}{\partial y} + \frac{\partial \tau_{xz}}{\partial z} = -\rho g \sin \alpha, \quad (1)$$

where τ_{xy} and τ_{xz} are the shear stresses, ρ is the density of ice, g the acceleration due to gravity, and α the inclination angle of the glacier surface (Fig. 1b). The z -component of the momentum balance yields a hydrostatic distribution of the pressure p . Glacial flow is treated as a non-Newtonian fluid, and Glen's flow law is used as a constitutive relation with the viscosity μ , so that

$$\frac{\partial u}{\partial y} = \frac{1}{\mu} \tau_{xy}, \quad \frac{\partial u}{\partial z} = \frac{1}{\mu} \tau_{xz}. \quad (2)$$

Equation (2) can be written as

$$\frac{\partial u}{\partial y} = 2F\tau_{xy}, \quad \frac{\partial u}{\partial z} = 2F\tau_{xz}. \quad (3)$$

The term F is the fluidity (here defined as one half of the inverse viscosity), which can be factorized as

$$F = A(\tau_e^2 + \tau_0^2)^{\frac{n-1}{2}}, \quad (4)$$

where τ_e is the effective stress, and the rate factor A and the flow-law exponent n are material parameters. We used the common values of $n = 3$ and $A = 214 \text{ MPa}^{-3} \text{ a}^{-1}$ (Paterson, 1994). The quantity τ_0 is introduced to avoid the mathematical singularity caused by an infinite viscosity when stresses approach zero (Blatter, 1995).

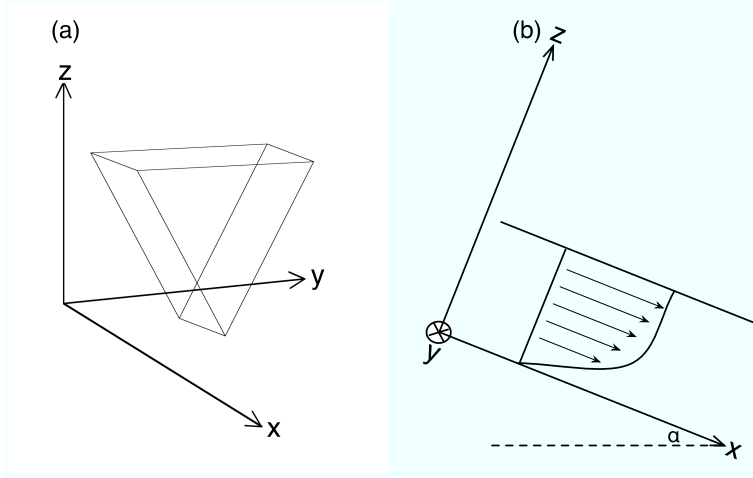


Figure 1: (a) Initial valley geometry and coordinate system used in the simulations. (b) Longitudinal glacier profile.

The boundary condition on the free surface ($z = S$) consists of vanishing pressure and shear traction,

$$p_s = 0, \quad \tau_s = \tau_{xz} = 0. \quad (5)$$

At the glacier base ($z = B(y)$), we introduce the basal sliding by linearly relating the sliding speed u_b to the shear stress acting on the bed τ_b (Weertman, 1964; Lliboutry, 1968, 1979),

$$u_b = -c \tau_b, \quad (6)$$

and

$$\tau_b = n_y \tau_{xy} + n_z \tau_{xz}, \quad (7)$$

$$n_y = \frac{1}{\sqrt{1 + \left(\frac{\partial B}{\partial y}\right)^2}} \frac{\partial B}{\partial y}, \quad n_z = -\frac{1}{\sqrt{1 + \left(\frac{\partial B}{\partial y}\right)^2}},$$

where $c = 50 \text{ m a}^{-1} \text{ MPa}^{-1}$ is our standard value of the sliding coefficient, which is constant across the glacier bed and has been chosen to obtain values for sliding velocity that allow for glacial erosion. The flow speed at the side margins is constrained to be zero.

The ice flow model was coupled with an erosion model by introducing a quadratic function of the sliding speed for the calculation of the erosion rate. Although the complex nature of the glacial erosion has not allowed the development of physically complete models for processes such as glacial abrasion, plucking, subglacial fluvial erosion, and chemical dissolution by subglacial water, this assumption for the erosion law represents the general form of the abrasion law proposed by Hallet (1979). Therefore, in the simulation described here, erosion rate normal to the bedrock surface was calculated as

$$E = C u_b^2, \quad (8)$$

where C is an erosion constant equal to 10^{-4} a m^{-1} (Harbor, 1992; MacGregor and others, 2000).

3 Numerical procedure

We prescribe a V-shaped cross section with maximum ice thickness of 480 m, surface width of 1200 m, and downglacier slope of 4° (Fig. 2a) as the initial glacier and valley geometries. We employ a two-dimensional finite-difference grid with 34×35 points to solve Eq. (1) for the flow speed within this cross section. The model solves a set of finite-difference equations with the LU factorization method assuming that the fluidity is constant and that the sliding speed is zero. To solve numerically Eq. (4) for the fluidity, a Newton-Raphson scheme is employed, and the computed velocity field is used so that the new values of the fluidity are utilized in the next iteration step. The velocity field is also utilized to compute the stress field with Eq. (3) to introduce sliding speed in the next step using Eq. (6). The computation is iterated until the velocity field converges within $2 \times 10^{-4} \text{ m a}^{-1}$.

Coupling the ice-flow model and the erosion model allows for investigating the temporal evolution of glacial valleys. For the first time step, the above procedures are used to calculate a flow pattern for the initial V-shaped valley. With the calculated basal sliding speeds, Eq. (8) is used to compute the pattern of erosion rate across the profile. Then the new coordinates for the glacier and the valley cross section are calculated and used for the next time step. The ice surface elevation is recalculated for each time-step by assuming a constant cross-sectional ice area. Consequently, in order to exclude ice-free points in the valley profile that emerge during the simulation due to the lowering of the ice surface, we allow the horizontal grid to shrink when the new finite-difference grid is regenerated for the new cross section. These procedures are repeated for a given number of time steps.

For all simulations carried out in this study, the simulation time scale is 50 ka with a time step of 1 ka, and it is assumed that there is no climate forcing that constrains the growth or the decline of the glacier.

4 Results and discussion

4.1 Full two-dimensional model vs. shallow-ice model

As stated in the introduction, the first motivation of this work is to investigate the glaciological conditions favorable to the development of U-shaped valleys. We are interested in

the investigation of the stress conditions that are required for the development of glacial valleys, and more precisely for the gradual transformation of the V-shaped pre-glacial valley to a U-shaped profile.

Figures 2a and 2b show the two-dimensional velocity field computed with the model described in Sect. 2 and the cross-sectional sliding velocities and erosion rates (for the initial V-shaped valley). Characteristic features of the sliding velocity and the erosion rate are the increase toward the interior of the glacier, but with local minima at the center of the cross profile. The increase of drag (whose origin is discussed later in this section) associated with the tight form at the center of the V-shaped valley reduces velocities there (Fig. 2b), resulting in a central minimum of the erosion (required to convert a V-shaped valley to a U-shaped channel). Figures 2a-l show the complete development sequence of a pre-glacial V-shaped valley to a recognizable U-shaped profile over 50 ka, and the associated sliding velocities and erosion rates every 10 ka. The model predicts the evolution of the V-shaped profile into a recognizable glacial form with sliding velocities ranging from 6 m a⁻¹ to 7 m a⁻¹, and for the last time-step, the model could simulate the formation of a deep and well-defined U-shaped valley (Fig. 2k).

Although the time scale is sensitively dependent on the value of the erosion constant in the erosion law, the model suggests that a glacial valley can be developed after 50 ka or during a single glaciation under the condition of realistic sliding speed. This observation agrees with previous results from Harbor (1992). As the valley is progressively transformed into a U-shaped form, the central minima in velocity and erosion rates gradually decrease and practically disappear during the last time-step (Fig. 2l).

For comparison with the full two-dimensional model, we now run a shallow-ice model that does not compute the lateral shear stress. The shallow-ice model only computes the shear stress parallel to the bed, therefore omitting the first term in Eq. (1), and by integration of the simplified equation, the basal shear stress is

$$\tau_b = -\tau_{xz}(z = B) = -\rho g H \sin \alpha, \quad (9)$$

where H is the ice thickness. We run the shallow-ice model with the same simulation procedure and initial setting as the full two-dimensional model. As shown in Fig. 3b, the pattern of the sliding velocity for the initial V-shaped profile is directly proportional to the ice thickness. Due to the nature of the erosion law, erosion values follow the same pattern. This pattern of erosion was applied to the initial V-shaped valley and Fig. 3c shows the glacial valley eroded during 50 ka. As observed, the valley shape remains similar to a V-shaped profile, characterized by a deep and narrow channel at the valley center. Clearly the ice thickness dependent basal shear stress in the shallow ice model results in higher velocities and erosion rates at the valley center because this stress configuration ignores the side walls effect on the ice flow and therefore prevents the development of a U-shaped profile. Harbor (1992) and our full two-dimensional model have clearly identified the friction effect that decreases the sliding velocity at the center of the V-shaped profile. In glaciological terms, the minimum basal velocity at the valley center is the consequence of the high drag between the narrow side walls, which reduces the deformation by shear at this location. The associated minimum erosion at the profile center leads to the gradual transformation of the V-shaped profile into a U-shaped form, the maximum of erosion being transferred closer to the valley margins. This process allows the profile to widen

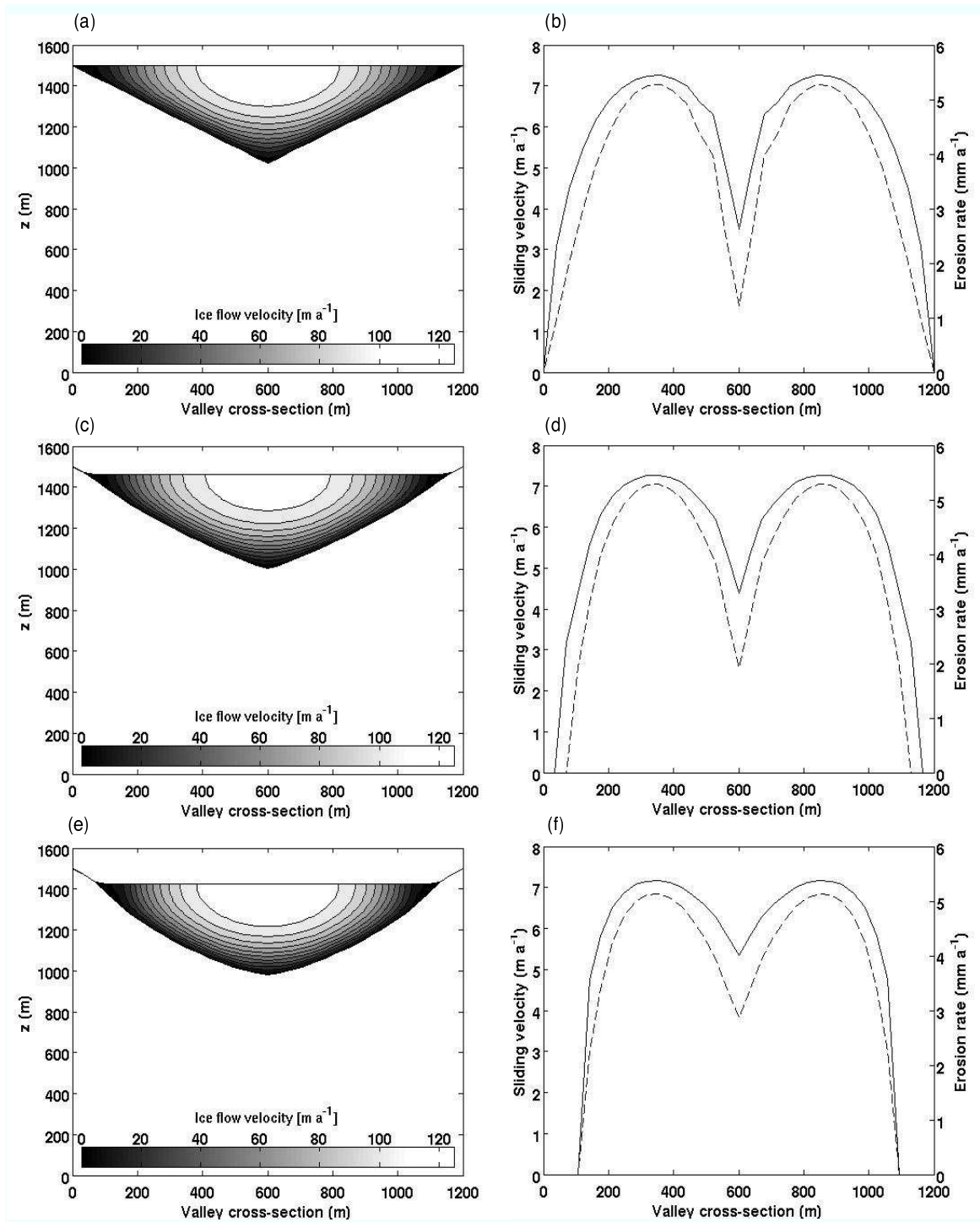


Figure 2: (a), (c), (e), (g), (i), (k) Glacial valley evolution from an initial pre-glacial profile computed with the two-dimensional model for times $t = 0, 10, 20, 30, 40$ and 50 ka. (b), (d), (f), (h), (j), (l) Corresponding cross-glacier variation of sliding velocities (solid lines) and erosion rates (dashed lines).

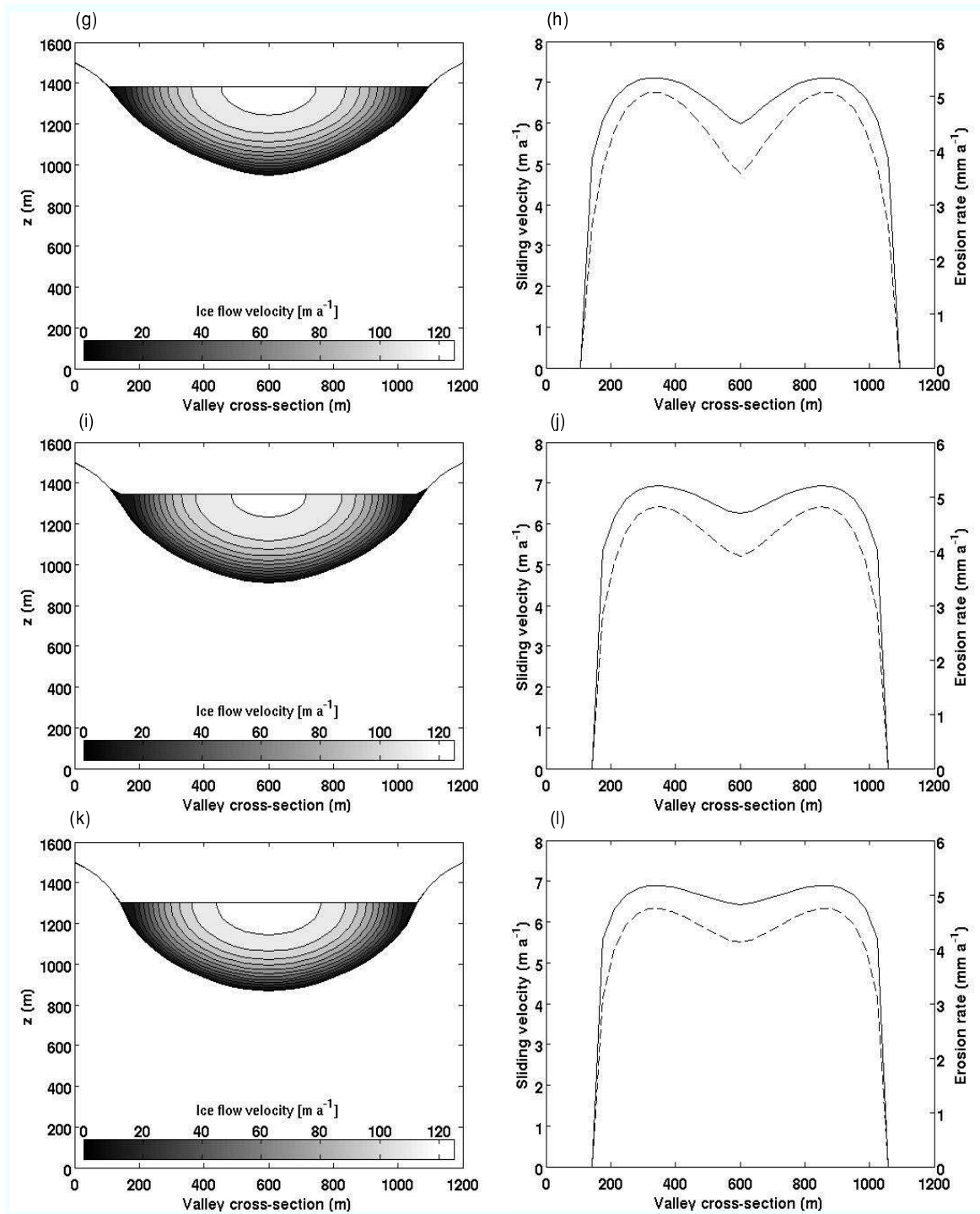


Figure 2: [cont.] (a), (c), (e), (g), (i), (k) Glacial valley evolution from an initial pre-glacial profile computed with the two-dimensional model for times $t = 0, 10, 20, 30, 40$ and 50 ka. (b), (d), (f), (h), (j), (l) Corresponding cross-glacier variation of sliding velocities (solid lines) and erosion rates (dashed lines).

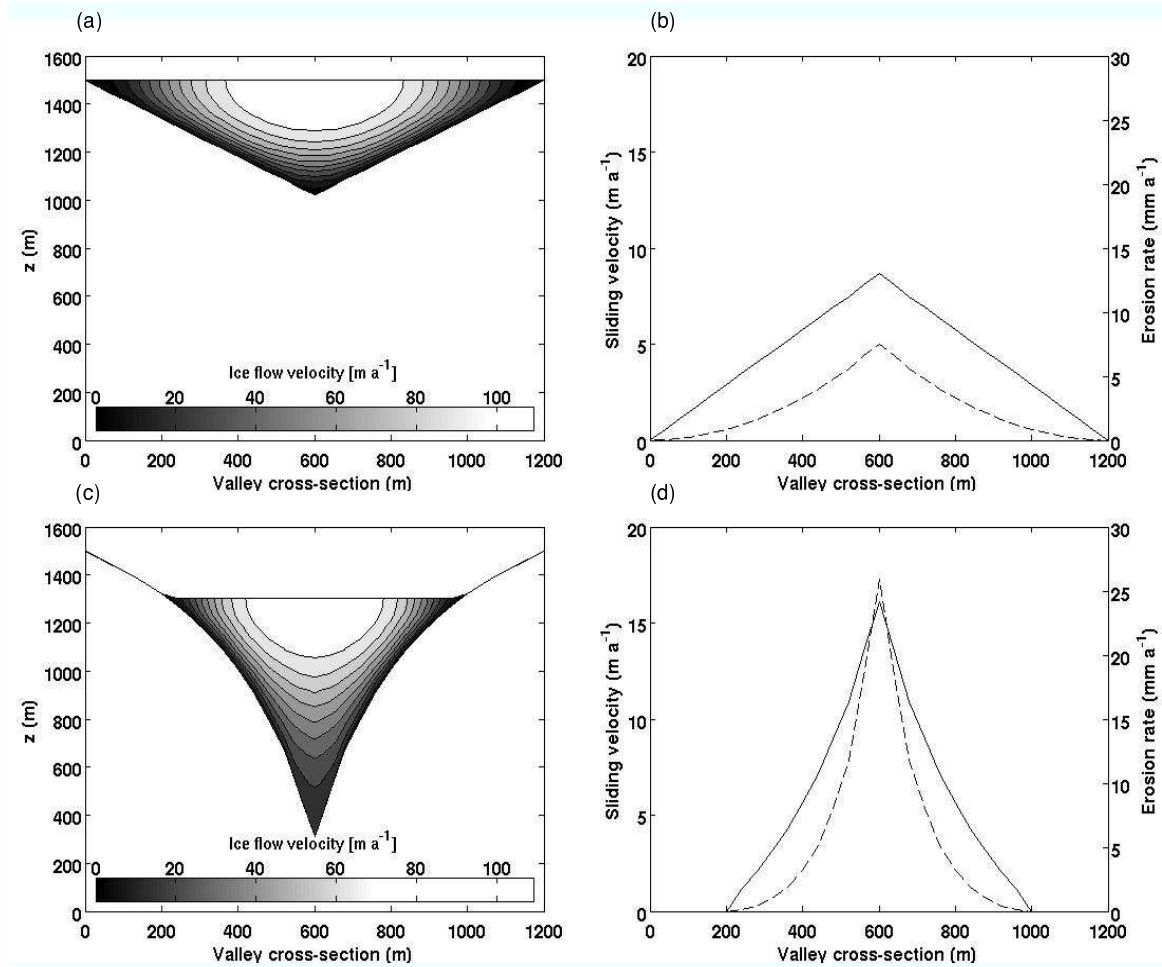


Figure 3: (a), (c) Initial V-shaped valley and eroded valley obtained with the shallow-ice model. (b), (d) Corresponding cross-glacier variation of sliding velocities (solid line) and erosion rates (dashed line).

toward a glacial valley shape. In the case of the shallow-ice model, such a process did not appear (Fig. 3d) and the resulting eroded valley still exhibits a V-shaped form.

The shallow-ice model allows us to compare the results computed with the full two-dimensional flow model in order to identify the primary factor of the drag effect described by Harbor (1990, 1992). This comparison shows clearly the importance of the lateral shear from the side walls, i.e., τ_{xy} , for the modeling of glacial erosion in a valley cross section. Ultimately, inclusion of both shear stress components τ_{xy} and τ_{xz} is necessary to obtain the sliding velocity pattern required for U-shaped valley formation.

4.2 Comparison with field data

Together with our motivation for the investigation of the stress conditions for glacial valley development, comparison with field data is needed for model validation. To describe the differences in morphology between valley profiles and in many glacial valley studies (Svensson, 1959; Harbor, 1992; Hirano and Aniya, 1988), it has been common to use a

power law equation as a mathematical function to represent the glacial trough cross-profile. The power law function is written as

$$z = ay^b, \quad (10)$$

where y and z are the horizontal and vertical distances from the lowest point of the cross section, and a and b are constants. The value b is commonly used as an index of the steepness of the valley side, and a a measure of the breadth of the valley floor. Previous studies suggested that the valley morphology progressively approaches a true parabolic form with increasing glacial erosion, and that stage of valley evolution can thus be measured by the proximity of b to 2 (Svensonn, 1959; Graf, 1970; Hirano and Aniya, 1988). For further comparison, we also use a form ratio FR , calculated by

$$FR = \frac{D}{W}, \quad (11)$$

where D is the valley depth and W is the valley top width. A large value of FR depicts then an overdeepening development of the glacial valley.

Only a few data describing present glacial valley shapes are available, and studies that try to determine the time scale for their formation by field measurements and profile reconstruction are still lacking. Consequently, our comparison will focus on investigating the shape of the glacial valley computed by the model and the shape measured in natural valleys. This is particularly useful in order to examine the sliding velocity values required to obtain a profile shape closed to the measured one. For our comparison work, we use the field measurements obtained by Yingkui and others (2001) in the Tian Shan Mountains, because they provide a rich set of form coefficient values calculated for several measured profiles. As described in their study, the morphological characteristics of glacial valley cross sections in the middle and western Tian Shan Mountains is represented by large variations of power law coefficients. Values of b in these areas range from 1.027 to 3.503, with most values in range 1.3-2.5. The average FR values of tributaries are commonly larger than those for the main valleys in these areas.

For our comparison study, our focus is the calculation of the exponent b and the form ratio FR values for the valley profile computed by the model, therefore the calculation of the value of a in Eq. (10) is ignored. We run the model with several values of the sliding coefficient c (from 10 to 50 $\text{m a}^{-1} \text{MPa}^{-1}$) used in the sliding law [Eq. (6)], in order to constrain the glacier sliding velocity. To ensure the convergence of the velocity field during the computation, we use several grid resolutions ranging from 34×35 to 94×95 points. Figure 4a shows the comparison between the b values provided by Yingkui and others (2001) for 48 profiles and those calculated with the computed profiles using different sliding coefficients, i.e., different sliding velocity conditions. As observed, the b values for the profiles computed by the model range from 1.13 to 2.05, and therefore they generally fit to the distribution of values observed by Yingkui and others (2001) where most values range from 1.3 to 2.5. More interestingly, the b values from the model results that fit most the general trend of the observed distribution are those where the sliding coefficient values are between 30 and 50 $\text{m a}^{-1} \text{MPa}^{-1}$. Consequently, a glacier with sliding velocities greater than 3-4 m a^{-1} would already be able to form a glacial valley shape similar to some observed valley profiles. Moreover, as it is usually assumed that a value

of 2 for the exponent b indicates a valley evolution that has reached a U-shape form, the model suggests that such form is obtained with sliding velocities greater than 6 m a^{-1} . As mentioned earlier, all the simulations have been run within 50 ka because 50 ka is a reasonable time-scale for the formation of the Tian Shan Mountains valleys during the last glacial period, even though the study by Yingkui and others (2001) did not provide a direct confirmation of this time scale. In that sense, our model results show that the formation within 50 ka of glacial valleys similar in shape to the Tian Shan mountains valleys is possible.

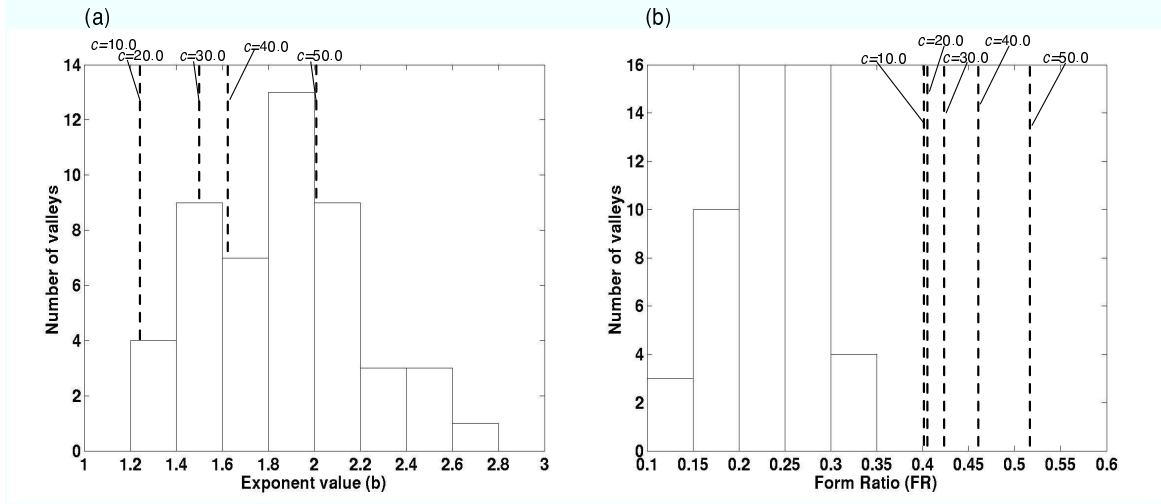


Figure 4: Comparison of the values of (a) the exponent b and (b) the form factor FR obtained with the model (dashed lines), and corresponding values obtained by Yingkui and others (2001) for the Tian Shan Mountains (histogram).

The comparison of the form ratio values obtained with the profiles computed by the model and those provided by field measurements is shown in Fig. 4b. We can clearly see that the general distribution trend of the form ratios between the model results and the measured profiles are significantly different. While the maximum values of FR provided by field data are close to 0.3, the results obtained by the model gives higher values ranging from 0.40 to 0.53. This is an important divergence of the models results from field data, as it indicates that the computed profile develops essentially by deepening without widening as opposed to the widening without deepening trend observed in the measured valleys. Better description of the development process of glaciated valley morphology can be addressed by describing the relationship between b values and form ratios within a ' b - FR diagram'. Hirano and Aniya (1988) have identified with their model two opposite trends in glacial valley development by analyzing the ' b - FR diagram' for several studied valleys. The Rocky Mountain model depicts an overdeepening development of the glacial valleys, and the Patagonia-Antarctica model indicates a widening rather than deepening process of the glacial valley development. Figure 5 shows the ' b - FR diagram' for the Tian Shan Mountains valleys and the model results computed with the sliding coefficients used in Fig. 4. The model results show larger b values with increasing form ratios (and increasing maximum velocities), as opposed to the data for the Tian Shan Mountains, which indicate smaller b values with increasing form ratios. For this reason, the measured valleys correspond to

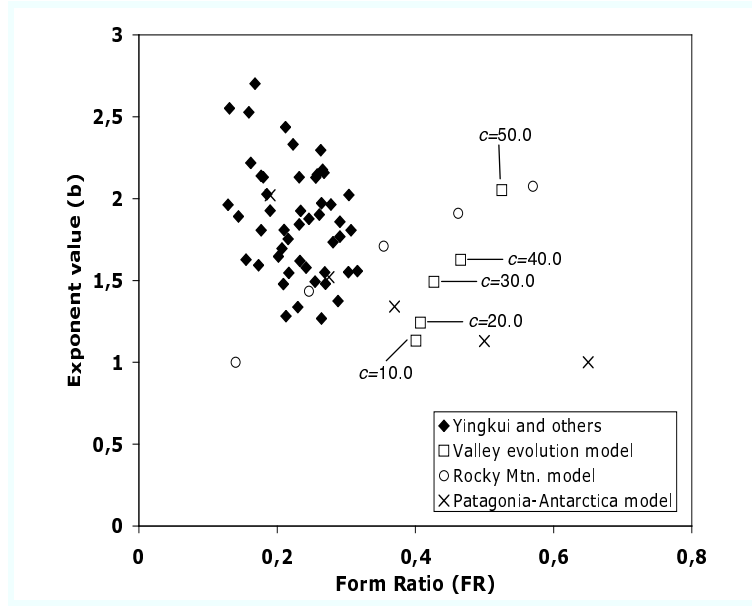


Figure 5: ‘ b - FR diagram’ for the glacial valley cross sections measured by Yingkui and others (2001) and for the profiles computed by the model with sliding coefficients c ranging from 10 to 50 $\text{m a}^{-1} \text{MPa}^{-1}$. The values for the Rocky Mountain and Patagonia-Antarctica models (Hirano and Aniya, 1988) are plotted for comparison.

the Patagonia-Antarctica model, whereas the model results show the similar trend of the Rocky Mountain model (Fig. 5). The difference in the glacial valley development processes usually reflects the difference in the initial V-shape of the valley, the initial relief, the ice thickness, the lithology and structure of the local rock and the glacial history. Although the V-shaped valley used as initial condition in the simulation could also explain why the computed profile only develops by deepening, the sliding velocity based erosion law is the main reason of this deepening. With increasing values of ice thickness, sliding velocities are higher and the erosion tends to be more important near the valley center, so that the valley deepening is faster than the widening. Consequently, as our model is not able to simulate the primary widening process observed in some glacial valleys, future investigations of glacial valley development modeling should focus on improving the erosion law. However, a sliding velocity based erosion model seems to be successful to simulate the Rocky Mountain model for the development process of glaciated valley morphology identified by Hirano and Aniya (1988). Running the model with a constant ice surface altitude and increasing ice volume gives the same pattern of valley development as previously described, i.e., development by deepening.

In order to investigate the possible influence of the sliding law in the erosion and in the development of glacial valleys, an alternative sliding law to the one described in Eq. (6) may be considered. For this purpose we use a sliding law which is also dependent on the effective pressure, so that the basal sliding is related to the basal shear stress τ_b and the effective pressure N by (Paterson, 1994)

$$u_b = k \frac{\tau_b^p}{N^q}, \quad (12)$$

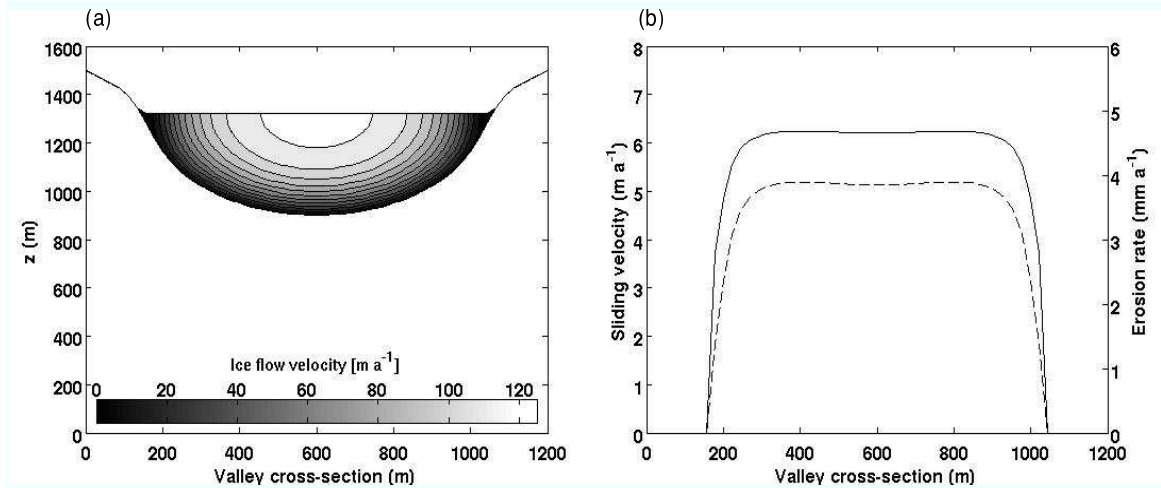


Figure 6: Model results obtained with the effective pressure included in the sliding law ($p = 3$, $q = 2$). (a) Glacial valley cross section at 50 ka. (b) Corresponding cross-glacier variation of sliding velocities (solid line) and erosion rates (dashed line).

where k is the sliding coefficient which is constant across the glacier bed, and p and q are constants equal to 3 and 2, respectively. The value of k is chosen in order to obtain sliding velocities in the range of those obtained in Fig. 2l. The effective pressure is defined by the ice overburden pressure p_i and the water pressure p_w as $N = p_i - p_w$.

We neglect the water layer, so that the effective pressure reduces to the ice overburden pressure. Figure 6 shows the developed glacial valley and the corresponding sliding velocities and erosion rates. Compared with Fig. 2l, the developed profile exhibits similar U-shaped topography, however calculated velocity and erosion values minima at the valley center have totally disappeared, suggesting that the U-shaped is more pronounced. This is confirmed by the b value (2.19), which is slightly higher than previously obtained in Fig. 4a (2.05 for $c = 50 \text{ m a}^{-1} \text{ MPa}^{-1}$). The FR value (0.5) is in the same range as in Fig. 4b (0.53). Therefore, the change in the sliding velocity law does not affect significantly the overall results presented in this paper.

5 Conclusion

This work presented a two-dimensional flow model of a glacier in a valley cross section, which has been coupled with an erosion law for the study of glacial valleys development. The model has successfully described the stress conditions inside the glacier required for the development of the glacial valley. Comparison with a shallow-ice model showed the importance of the lateral shear stress (lateral drag) in order to obtain the proper pattern of the sliding velocity and the erosion in the initial V-shaped valley for the development of the U-shaped profile.

Comparison with field data obtained in the Tian Shan Mountains allowed for constraining the value of the sliding coefficient in the basal sliding law so that such forms, i.e., U-shaped profiles, could be obtained within 50 ka. However, the process of formation of the Tian Shan Mountains valleys could not be simulated with our model. Notably,

different values for the form ratio compared with the measured valleys showed that the development of glacial valleys simulated with a sliding velocity based erosion law occurs by a deepening without widening process (Rocky Mountain model). However, the measured valleys have developed with a widening without deepening process (Patagonia-Antarctica model), which our model was not able to simulate due to the way the erosion law was defined.

Future improvements of the valley evolution model should focus on more comparisons with field data and on the enhancement of the erosion law. Improving the simulation of the erosion occurring at the valley margins should provide a better way to simulate valleys that correspond to the Patagonia-Antarctica model. Further, a three-dimensional model would certainly provide a better understanding of the evolution of the glacial valley cross section together with the evolution of the longitudinal profile.

Acknowledgements

We wish to extend our thanks to Heinz Blatter (Institute for Atmospheric and Climate Science, ETH Zurich) for providing useful lecture notes on glacier modeling, and to Jean-Luc Mercier (Faculty of Geography, Louis Pasteur University Strasbourg) for his comments and interest in this work. Furthermore, we are grateful to many colleagues at the Institute of Low Temperature Science for helpful discussions.

References

- Aniya, M. and Welch, R., 1981. Morphological analyses of glacial valleys and estimates of sediment thickness on the valley floor: Victoria Valley system, Antarctica. *The Antarctic Record*, **71**, 76–95.
- Bindschadler, R., 1982. A numerical model of temperate glacier flow applied to the quiescent phase of a surge-type glacier. *J. Glaciol.*, **28**, 239–265.
- Blatter, H., 1995. Velocity and stress fields in grounded glaciers: a simple algorithm for including deviatoric stress gradients. *J. Glaciol.*, **41**, 333–344.
- Budd, W.F. and Jensen, D., 1975. Numerical modeling of glacier systems. International Association of Hydrological Sciences Publication No. 104, 257–291.
- Doornkamp, J.C. and King, C.A.M., 1971. *Numerical Analysis in Geomorphology*. Edward Arnold, London, England, 608 p.
- Girard, W.W., 1976. Size, shape and symmetry of the cross-profiles of glacial valleys. Ph.D. thesis, Iowa City, Iowa, University of Iowa, 90 p.
- Graf, W.L., 1970. The geomorphology of the glacial valley cross-section. *Arctic and Alpine Research*, **2**, 303–312.
- Hallet, B., 1979. A theoretical model of glacial abrasion. *J. Glaciol.*, **23**, 39–50.
- Hallet, B., 1981. Glacial abrasion and sliding: Their dependence on the debris concentration in basal ice. *Ann. Glaciol.*, **2**, 23–28.
- Harbor, J.M., 1990. Numerical modeling of the development of glacial-valley cross sections. Ph.D. thesis, University of Washington, Seattle, Washington, 219 p.
- Harbor, J.M., 1992. Numerical modeling of the development of U-shaped valleys by glacial erosion. *Geological Society of America Bulletin*, **104**, 1364–1375.
- Harbor, J.M., 1995. Development of glacial-valley cross-sections under conditions of spatially variable resistance to erosion. *Geomorphology*, **14**, 99–107.

- Hirano, M. and Aniya, M., 1988. A rational explanation of cross-profile morphology for glacial valleys and of glacial valley development. *Earth Surface Processes and Landforms*, **13**, 707–716.
- Hooke, R.L., Raymond, C.F., Hotchkiss, R.L. and Gustafson, R.J., 1979. Calculation of velocity and temperature in a polar glacier using the finite-element method. *J. Glaciol.*, **24**, 131–146.
- Iken, A., 1981. The effect of the subglacial water pressure on the sliding velocity of a glacier in an idealized numerical model. *J. Glaciol.*, **27**, 404–421.
- Iverson, N.R., 1990. Laboratory simulations of glacial abrasion: Comparison with theory. *J. Glaciol.*, **36**, 304–314.
- Iverson, N.R., 1991. Potential effects of subglacial water-pressure on quarrying. *J. Glaciol.*, **37**, 27–36.
- Lliboutry, L., 1968. General theory of subglacial cavitation and sliding of temperate glaciers. *J. Glaciol.*, **7**, 21–58.
- Lliboutry, L., 1979. Local friction laws for glaciers: a critical review and new openings. *J. Glaciol.*, **23**, 67–95.
- MacGregor, K.R., Anderson, R.S., Anderson, S.P. and Waddington, E.D., 2000. Numerical simulations of glacial-valley longitudinal profile evolution. *Geol.*, **28**, 1031–1034.
- Mahaffy, M.W., 1976. A three-dimensional numerical model of ice sheets. Test on the Barnes Ice Cap, Northwest Territories. *J. Geophys. Res.*, **81**, 1059–1066.
- Nye, J.F., 1965. The flow of a glacier in a channel of rectangular, elliptic or parabolic cross-section. *J. Glaciol.*, **5**, 661–690.
- Oerlemans, J., 1984. Numerical experiments on large-scale glacial erosion. *Zeitschrift für Gletscherkunde und Glazialgeologie*, **20**, 107–126.
- Paterson, W.S.B., 1994. *The Physics of Glaciers*. 3rd edition, Pergamon Press, Oxford etc., 480 p.
- Reynaud, L., 1973. Flow of a valley glacier with a solid friction law. *J. Glaciol.*, **12**, 251–258.
- Shoemaker, E.M., 1988. On the formulation of basal debris drag for the case of sparse debris. *J. Glaciol.*, **34**, 259–264.
- Svenson, H., 1959. Is the cross-section of a glacial valley a parabola? *J. Glaciol.*, **3**, 362–363.
- Yingkui, L., Gengnian, L. and Zhijiu, C., 2001. Glacial valley cross-profile morphology, Tian Shan Mountains, China. *Geomorphology*, **38**, 153–166.
- Weertman, J., 1964. The theory of glacier sliding. *J. Glaciol.*, **5**, 287–303.